

h^u

STATISTICAL-THERMODYNAMIC THEORY OF SURFACTANT ORGANIZATION IN
MICELLES AND BILAYERS

A. Ben-Shaul¹, I. Szleifer¹ and W. M. Gelbart²

1. Department of Physical Chemistry and
The Fritz Haber Center for Molecular Dynamics
The Hebrew University, Jerusalem 91904, Israel

2. Department of Chemistry
University of California, Los Angeles, CA 90024

The probability distribution of chain conformations in micellar aggregates of arbitrary geometry is derived using two alternative approaches: (i) By minimizing the free energy functional of a single chain, subject to the packing constraints imposed by the presence of neighboring chains in the hydrophobic core; (ii) By expanding the many-chain configurational integral in terms of the excluded volumes characterizing one ('central') chain in a given conformation. The central assumption in both derivations is that chain organization and conformational statistics in amphiphilic aggregates are governed by the short-range, repulsive, inter-molecular interactions. Bond order parameter profiles and other single chain properties which can be calculated using the conformational probability distribution are in good agreement with experimental and computer simulation studies. Yet, our main concern in this paper is the theoretical (statistical thermodynamic) description of chain organization within the hydrophobic core, with particular emphasis on the role of micellar geometry. In this spirit a considerable part of the discussion is devoted to comparisons with other theoretical approaches.

INTRODUCTION

The hydrophobic cores of micellar aggregates and bilayers are often described as liquid hydrocarbon droplets.^{1,2} Experiments indicate that the density of the hydrocarbon chains within the cores is, indeed, liquid-like.^{1,3} On the other hand, because of the very special organization of the molecules in amphiphilic aggregates, their statistical thermodynamic properties are quite different from those in the bulk liquid and depend on the core's geometry. The main characteristics of this organization are: i) the anchoring of the polar head to the core-water interface, and ii) the microscopic scale (on the order of a chain length) of at least one dimension of the aggregate, e.g., the width of a bilayer. These 'boundary conditions' induce anisotropic chain ordering similar to that observed in alkanes dissolved in liquid crystalline solvents.⁴ Magnetic resonance experiments provide information on the extent of chain

ordering and reveal that it varies from one micellar geometry to another, indicating that chain statistics in micellar aggregates are, indeed, geometry dependent.^{5,6}

The statistical-thermodynamic aspects of chain organization in micelles, bilayers and interfaces are important for understanding the mechanisms of surfactant association, relative stability of various aggregate shapes, phase transitions in micellar solutions and microemulsions, solubilization of hydrophobic species in micelles and bilayers, and various other issues. Many theories have been formulated to describe the statistical thermodynamics of hydrocarbon chains in bilayer membranes, mainly within the context of the 'gel-liquid-crystal' phase transition.⁷ Recently, several theoretical studies have treated chain statistics above this transition. These include models based on (various) packing considerations,^{1,2,8,9} 'single-chain' ('mean field') theories¹⁰⁻¹⁸ and many-chain (Monte-Carlo and molecular-dynamics) computer simulations.¹⁹⁻²² The simulations can provide detailed information on molecular structure and dynamics. Yet, so far, only few studies of this kind are available and none of them have been applied to analyze the dependence of chain statistics on micellar geometry. This issue is explicitly considered by three 'single-chain' theories due to Gruen,¹¹⁻¹³ Dill et al.¹⁴⁻¹⁶ and the present authors.^{17,18} One advantage of such theories is that they provide simple expressions for the probability distribution of chain conformations and related quantities.

In addition to presenting our own theory, our major objective here is to compare it with the other two single-chain theories.¹¹⁻¹⁶ In the next section we present two alternative derivations of our (singlet) probability distribution function for chain conformations in aggregates of arbitrary geometries. A few representative results for simplified model chains are presented in section 3. Section 4 is devoted to a rather detailed comparison with the theories of Dill et al. and of Gruen.

PROBABILITY DISTRIBUTION OF CHAIN CONFORMATIONS

In the derivation presented below it will be assumed that: i) The chains within the hydrophobic core are packed at uniform, liquid-like, density; ii) The interface separating the core and the surrounding solution is smooth; and iii) the hydrophilic heads of the surfactants are always located in the solution -- just beyond the interface. This picture is supported by experiments and several theoretical studies.^{12,13,16} It neglects local density and surface (roughness) fluctuations which, according to some theoretical analyses, can be significant²¹ (especially in small 'spherical' micelles). These effects could be incorporated in our approach, in an approximate manner, but to keep the discussion simple they will not be included here. For the same reason the numerical examples presented below involve only three 'basic' micellar geometries: spheres, cylinders and planar bilayers. Other shapes such as ellipsoids or vesicles can be treated similarly.

A convenient way to specify the micellar geometry is to divide the core into several layers, parallel (or concentric) to the hydrocarbon-water interface. We use M_i to denote the volume of layer i , with $i = 1, \dots, L$ numbering the layers from the interface towards the center of the micelle (or the mid-plane in bilayers), as in Figure 1. Although other choices are possible¹¹⁻¹³ we assume all layers to have the same width, ΔL (except, in some cases, the innermost layer). The choice of ΔL is arbitrary. In Figure 1 it is set equal to one bond length of the 'cubic' model chain. The radius (half-thickness) of the hydrophobic core is measured by L . The curvature is specified by the i -dependence of M_i . $M_i = M_1 = \text{constant}$ for

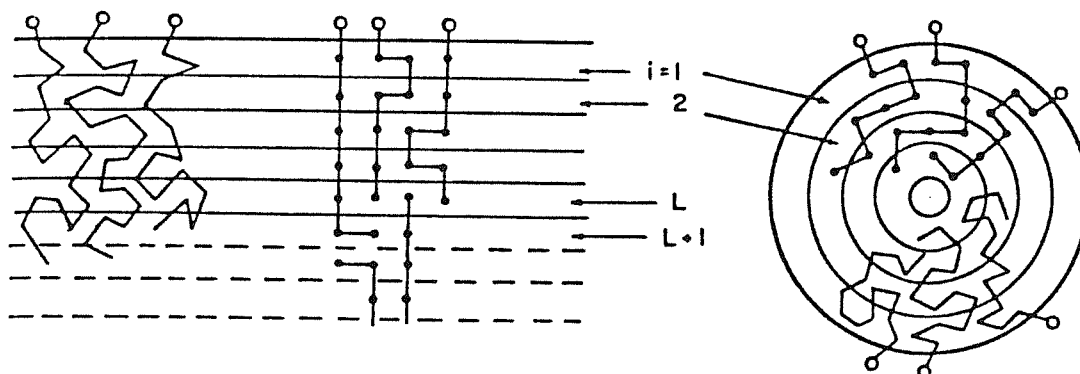


Figure 1: A schematic two dimensional representation of surfactant chains in planar bilayers (left) and curved (spherical or cylindrical) micelles (right). The theory described in the text is applicable to any chain model. The figure shows two types of chains: i) 'cubic' (i.e., 0 or $\pi/2$ bond angles), ii) more realistic 'rotational-isomeric-state' chains with nearly tetrahedral bond angles. The results shown in Figures 2, 3 below are for the cubic chains and those in Figure 4 for the 'realistic' chains. The figure illustrates a 'central' chain surrounded by neighboring chains.

planar bilayers. For spheres and cylinders, $M_i/M_1 = (L-i)^2$ and $(L-i)$, respectively. (Of course, in the calculations^{17,18} we use the exact values of M_i .) Note that M_1 is proportional to the surface area of the aggregate.

Let $P(a)$ denote the (singlet) probability distribution function (pdf) of chain conformations, i.e., $P(a)$ is the probability of finding a chain in conformation a . The symbol a is used to denote the sequence of internal bond angles of the chain as well as the position of the polar head and the orientation of the chain with respect to the interface. The allowed conformations are those for which all chain segments are confined to the inner side of the interface. Consequently, their number depends on the geometry of the core. Yet, this dependence plays only a marginal role in determining the statistical properties of the chains, e.g., their bond order parameter profiles. The statistical weights of the various conformations depend as well on their internal ('gauche-trans') energies, $\epsilon(a)$. But, as we shall see below, the geometry dependence of $P(a)$ is governed primarily by the packing constraints on the chains.

Molecular packing in liquids is mainly determined by the short-range repulsive forces between the molecules.²³ Based on this notion and the assumption that the density in the hydrophobic core is uniform and liquid-like, we shall assume that the only intermolecular forces determining $P(a)$ are short range repulsions between neighboring chains. More specifically, the repulsive forces will be treated as hard-core (excluded volume) interactions, i.e., the chains are regarded as semi-flexible hard particles. In this ('van der Waals-type') picture, the long-range interactions are represented by a uniform attractive potential background which is the same for all possible organizations (a_1, a_2, \dots, a_N) of the N chains packed in the core. Note that in lattice models this assumption is automatically satisfied if all sites are occupied.

Let n denote the number of chain segments (e.g., CH_2 groups in alkyl chains) and v the average volume per chain in the the bulk liquid. The quantity $v = v/n$ will be identified with the 'hard core' volume per segment. Let $\phi_i(a)$ denote the volume occupied in layer i by a chain in conformation a . Our assumption of uniform and liquid-like density in the hydrophobic core implies^{17,18}

$$\phi_i(a_1, \dots, a_N) = \sum_{j=1}^N \phi_i(a_j) = M_i, \quad i = 1, \dots, L \quad (1)$$

where ϕ_i is the total volume occupied by the N chains in layer i . (As mentioned previously, our formulation can be generalized to non-uniform and lower densities than that of the bulk liquid. In these cases (1) is replaced by $\phi_i \leq M_i$ ¹⁸). There are many 'organizations' a_1, \dots, a_N consistent with the 'volume filling' condition (1). For any single chain, this implies $\langle \phi_i \rangle = M_i/N$ or, more explicitly,

$$\langle \phi_i(a) \rangle = \sum_a P(a) \phi_i(a) = m_i \quad i = 1, \dots, L \quad (2)$$

where $m_i = M_i/N$ is the average volume available per chain in layer i . $P(a)$ is the singlet pdf obtained from the joint (many-chain) distribution $P(a_1 = a, a_2, a_3, \dots, a_N)$ by summing over a_2, \dots, a_N , i.e. (2) follows from (1) by multiplying both sides of the second equality in (1) by $P(a_1, \dots, a_N)$ and summing over all a_j .

Since the volume of the chain ($v = nv$) is fixed, $\sum_i \phi_i(a) = nv$ regardless of a . Hence

$$\begin{aligned} \sum_{i=1}^L \langle \phi_i(a) \rangle &= \sum_{i=1}^L \sum_a P(a) \phi_i(a) \\ &= \sum_a P(a) \sum_{i=1}^L \phi_i(a) = nv \end{aligned} \quad (3)$$

where we have used the normalization condition $\sum_a P(a) = 1$. Thus, from (2) and (3)

$$\sum_{i=1}^L m_i = \sum_{i=1}^L M_i/N = M/N = nv \quad (4)$$

which is simply the requirement for volume filling ($M = Mnv$).

Because of (3), or equivalently (4), only $L-1$ of the L conditions (2) are linearly independent. These conditions represent packing constraints on $P(a)$. Their geometry dependence is reflected by the i -dependence of the m_i 's. In particular, m_1 is proportional to the average area per head-group at the core-water interface, which is a central parameter in all theories of amphiphile self-assembly.^{1,2}

Equation (2) accounts for the constraints imposed on a given chain by the 'mean field' due to its neighbors. The free energy of the chain as a functional of $P(a)$ is

$$\begin{aligned} \tilde{A} &= \tilde{E} - T\tilde{S} \\ &= \sum_a P(a) \epsilon(a) + kT \sum_a P(a) \ln P(a) \end{aligned} \quad (5)$$

where \tilde{X} , ($X = A, E, S$, etc.) represents a (mean field) thermodynamic

quantity per chain. (Note that the formulation leading up to equation (5) assumes that the mean field is due to steric repulsions from the chain excluded volumes rather than to dispersional attractions between chains; this is consistent with our taking the hydrocarbon density to be constant throughout the micellar core). $\epsilon(a)$ is the internal energy of the chain and k is Boltzmann's constant. According to the maximal entropy formalism (information theory approach) the 'most likely' pdf of any system is the one which minimizes the free energy of this system subject to the appropriate constraints.²⁴ In our case the system is a single chain surrounded by many others and the constraints are the packing conditions (2). (The above statement is a special case of the maximal entropy principle appropriate for a system in contact with a thermal bath. It follows from the more general principle which requires maximization of S , provided $E = \langle \epsilon \rangle = \int P(a)\epsilon(a) = \text{constant}$ is regarded as an additional constraint.) The maximal entropy approach yields all the familiar distribution functions in statistical thermodynamics, e.g., the canonical, microcanonical and grand-canonical distributions. We shall use it to derive $P(a)$; then we obtain the same expression by a different approach.

Finding the pdf which minimizes \bar{A} subject to (2) is a standard procedure which yields

$$P(a) = \frac{\exp[-\beta\epsilon(a) - \sum_1 \lambda_i \phi_i(a)]}{z'}$$

$$= \frac{\omega(a) \prod_1 \alpha_i^{\phi_i(a)}}{z'} \quad (6)$$

where $\omega(a) = \exp[-\beta\epsilon(a)]$, $\alpha_i = \exp(-\lambda_i)$ and $\beta = 1/kT$. The partition function z' ensures that $P(a)$ is normalized. λ_i are the Lagrange parameters associated with the $\langle \phi_i \rangle$. They are determined by substituting $P(a)$ into (2). (To keep α_i and ϕ_i dimensionless, ϕ_i should be measured in units of v and λ_i in units of $1/v$.) Recall that because of (3) only $L-1$ of the L constraints are linearly independent. This implies that one of the λ_i 's (or α_i 's) may be chosen arbitrarily. In our calculations we have always set $\lambda_L = 0$ ($\alpha_L = 1$). (To verify that this is allowed, substitute $\phi_L(a) = nv - (\phi_1(a) + \dots + \phi_{L-1}(a))$ in (6). The factor $\exp(-nv\lambda_L)$ will cancel out as it also appears in z' and all λ_i will be replaced by $\lambda_i - \lambda_L = \lambda_i$. Since $P(a)$ is uniquely specified by the λ_i , the value of λ_L is irrelevant).

Substituting (6) into (2), we obtain the equations determining the λ_i 's (α_i 's):

$$-\frac{\partial \ln z'}{\partial \lambda_i} = \frac{\partial \ln z'}{\partial \ln \alpha_i} = m_i \quad (7)$$

or, more explicitly,

$$\sum_a [\phi_i(a) - m_i] \omega(a) \prod_j \alpha_j^{\phi_j(a)} = 0 \quad i = 1, \dots, L-1 \quad (8)$$

In all our calculations the α_i 's have been determined by a numerical solution of the nonlinear algebraic equations (8). (The form (7) is useful only if z' can be evaluated in a closed form. In our problem this is not the case unless drastic approximations are imposed on $P(a)$.)

The quantities, π_i , defined by

$$\pi_i = kT\lambda_i \quad (9)$$

have the dimensions of pressure, cf. (6) or (7). Since they vary from one layer to another, they will be called 'lateral pressures'.^{11-13,25} Using (5), (6) and (7), it can be shown directly that the π_i 's have the significance of pressure.¹⁸ This assertion will become more apparent from our alternative derivation of expression (6) for $P(a)$, as outlined next.

Consider a micellar aggregate (fixed in space and orientation) in which all chain-heads are anchored to fixed positions at the interface. For the sake of concreteness, suppose that these are the equilibrium positions (see below). The probability of finding the chains in organization a_1, \dots, a_N is given by¹⁸

$$P(a_1, a_2, \dots, a_N) = \frac{1}{Z} \exp[-\beta V(a_1, \dots, a_N)] \quad (10)$$

where V is the overall potential energy of the chains in the core and Z is the configurational sum

$$Z = Z(N, T, M_i) = \sum_{a_1, \dots, a_N} \exp[-\beta V(a_1, \dots, a_N)] \quad (11)$$

where by M_i we denote the set $\{M_i\}$. The geometry, i.e., the M_i -dependence of Z , enters via the boundary conditions on the allowed conformations (corresponding formally to $V = \infty$ whenever any chain segment protrudes beyond the interface). Note that Z is a canonical partition function, i.e.,

$$A = -kT \ln Z \quad (12)$$

is the (configurational) Helmholtz free energy of the chains.

Since the polar heads are assumed to be fixed, the interaction energy between them is a constant, independent of a_1, \dots, a_N . Similarly, the interaction between the solvent and those portions of the chains in contact with it is also independent of a_1, \dots, a_N , because the interface is assumed to be smooth. These constant 'surface' contributions are not included in V . As discussed earlier, the attractive long-range parts of the inter-chain potential are assumed to constitute a constant background contribution to V , which can be set equal to zero as it does not affect $P(a_1, \dots, a_N)$. Thus V can be expressed as

$$\begin{aligned} V^{(N)}(a_1, \dots, a_N) &= \sum_{j=1}^N \epsilon(a_j) + U^{(N)}(a_1, \dots, a_N) \\ &= \sum_{j=1}^N \epsilon(a_j) + \sum_{j < l}^N u(a_j, a_l) \end{aligned} \quad (13)$$

where the first sum involves the internal ('trans-gauche') energies of the chains. $U^{(N)}$ represents the hard-core repulsive potential between segments belonging to different chains. In the second line of (13) $U^{(N)}$ is expressed as a sum of hard-core pair potentials, i.e., $u(a_j, a_l) = \infty$ or 0 depending whether the chains do, or do not, overlap each other, respectively.

Substituting (13) into (10) and summing over a_2, \dots, a_N , we obtain the singlet distribution $P(a_1) = P(a)$,

$$P(a_1) = \sum_{a_2, \dots, a_N} P(a_1, \dots, a_N) \quad (14)$$

$$= \frac{1}{Z} \exp[-\beta \epsilon(a_1)] \left\{ \sum_{a_2, \dots, a_N} \exp[-\beta \sum_{j \neq 1} u(a_1, a_j)] - \beta V^{(N-1)}(a_2, \dots, a_N) \right\}$$

with $V^{(N-1)}$ defined as in (13). The factor $\exp[-\beta \sum u(a_1, a_j)]$ vanishes whenever any one of the chains $2, \dots, N$ overlaps chain 1 and is 1 otherwise. Hence, the sum in the curly brackets is the configurational partition function of a system containing $N-1$ chains in a volume of shape defined by (M_i) , except that it is denied the volume occupied by chain 1. The volume taken up by chain 1 in layer i is $\phi_i(a_1)$, implying that the volume available to the other $N-1$ chains, in this layer, is $M_i - \phi_i(a_1)$. Hence, the sum in the curly brackets is $Z(N-1, T, M_i - \phi_i(a_1))$, provided we assume that only the volume, $\phi_i(a_1)$, excluded to the $N-1$ chains--and not the exact shape of a_1 --determines the partition function. Based on these arguments we can write

$$P(a) = \exp[-\beta \epsilon(a)] Z(N-1, T, M_i - \phi_i(a)) / Z(N, T, M_i) \quad (15)$$

Taking the logarithm of this equation and expanding $\ln Z(N-1, T, M_i - \phi_i(a))$ around N, T, M_i we find

$$\ln P(a) = -\beta \epsilon(a) - \left(\frac{\partial \ln Z}{\partial N} \right)_{T, M_i}$$

$$- \sum_i \left(\frac{\partial \ln Z}{\partial M_i} \right)_{N, T, M_{j \neq i}} \phi_i(a) + O\left(\frac{1}{N}\right) \quad (16)$$

The higher order terms are $O(1/N)$ because $\ln Z$, being the aggregate's free energy, is proportional to N , and $M_i = Nm_i$. (For spheres, this is an approximation. With $\ln Z \propto N$ we actually refer to sections of the sphere.) Neglecting the $O(1/N)$ terms we notice that (16) is identical to (6) with

$$\beta \pi_i = \lambda_i = \frac{\partial \ln Z}{\partial M_i} = -\beta \frac{\partial A}{\partial M_i} \quad (17)$$

and

$$\ln z' = \left(\frac{\partial \ln Z}{\partial N} \right)_{T, M_i} = -\beta \left(\frac{\partial A}{\partial N} \right)_{T, M_i} \quad (18)$$

where we have also used (9) and (12). Equation (17) clearly demonstrates that the name 'lateral pressure' associated with π_i is based on physical reasoning rather than semantics: π_i is a measure of the free energy change associated with a change in the 'lateral volume' M_i .

Since $\ln Z(N, T, M_i)$ is extensive, it must be proportional to N . The proportionality factor, which will be denoted as $\ln z$, is a function of the intensive variables T and $m_i = M_i/N$. Namely,

$$\ln Z(N, T, M_i) = N \ln z(T, m_i) \quad (19)$$

Note that $\ln z'$ as (implicitly) defined by (6), or (16) and (18), is a function of T and the π_i 's. Using (17), (18), (19) and the definition $M_i = Nm_i$, it can be verified that

$$\ln z' = \ln z - \beta \sum_i \pi_i m_i \quad (20)$$

showing that $\ln z'$ and $\ln z$ are related by a Legendre transformation, just like the Helmholtz and the Gibbs free energies. In fact, since the sum in (20) is simply a generalized "PV" term, $\ln z'$ and $\ln z$ represent, respectively, the Gibbs and Helmholtz free energies per chain. Indeed, from (18), $-kT \ln z'$ is the chemical potential of a molecule in the aggregate (i.e., the Gibbs free energy per molecule). Moreover, using (2), (6) and (20), it is easily shown that, cf. (5),

$$\bar{A} = -kT \ln z(T, m_1) \quad (21)$$

This quantity is the average Helmholtz free energy per molecule in the aggregate, (more precisely--the configurational contribution to this quantity). Hence, \bar{A} is the chain-conformational contribution to the standard chemical potential of the aggregate--a central quantity in the theory of micelle formation and growth.

In the second derivation of $P(a)$, it has been assumed that the polar heads are held fixed at the interface. This approximation allowed us to treat the head-group interaction terms as constants, independent of chain organization within the core. Nowhere in the derivation was it needed to specify exactly how the heads are distributed over the interface. This is because what we have actually assumed is that chain interactions and head-group interactions are separable. Clearly, this is an approximation, but a reasonable one, for two reasons. First, at least for charged surfactants, the strong electrostatic repulsions will tend to localize the heads within a narrow region around their equilibrium positions. Second, since $P(a)$ reflects the average properties of all chains, correlations between head-group distances and chain conformation statistics may be expected to play a minor role. Of course, only detailed calculations can provide a definite answer. Yet, it should be remembered that various other approximations (e.g., surface smoothness) should be examined simultaneously.

NUMERICAL EXAMPLES

In this section, we present the results of some calculations based on the theory developed in the previous section. The presentation will be illustrative rather than exhaustive. The calculations discussed here were carried out for the 'cubic' model chains shown in Figure 1. Hence, we have not attempted any detailed comparisons with experimental data. It should be noted, however, that all the results show good qualitative agreement with available experimental and computer simulation data. In the next section it is demonstrated that when our $P(a)$, cf. (6), is applied to the more realistic (tetrahedral, rotational-isomeric-state) chain model the agreement with such data is excellent (i.e., quantitative).

Each segment of the model chains in Figure 1 represents 3.6 CH_2 groups of real alkyl chains. This choice has been suggested by Dill and Flory because the diameter of an alkyl chain (as inferred from liquid hydrocarbon density data) is equal to a 3.6 bond-long segment of an (all trans) n -alkane chain.¹⁴ Hence, the chain density of a cubic lattice--fully packed with such segments--is equal to that of a bulk liquid hydrocarbon. Note, however, that the theory presented in the previous section does not require a lattice and that it is valid for any chain model.

The internal energy of the model chains is expressed as $\epsilon(a) = k(a)\chi$ where $k(a)$ is the number of 'kinks' ($\pi/2$ angle between adjacent bonds) in conformation a , and χ is the kink energy. This implies $\omega(a) = \gamma^{k(a)}$ with $\gamma = \exp(-\beta\chi)$. The value of γ was determined by requiring that the mean end-to-end distance of a single, isolated, chain be equal to that of a

corresponding alkyl chain represented by the rotational isomeric state model.^{26,27} This criterion was adopted from reference 21. It ensures that in the absence of packing constraints the real and model chains have similar dimensions. The value obtained in this way for γ was 0.3 (almost independently of chain length, for alkyl chains containing 10-25 carbon atoms). The 'zeroth' bond, connecting the head group with the first chain segment, is not equivalent to the internal bonds. Consequently, a kink between the zeroth and the first bond was assigned a statistical weight γ_h which was treated as a parameter. The properties of the chains are insensitive to the choice of this parameter, except the order parameters of the first two bonds, but even here the effect is small. In the results presented below we have used $\gamma_h = 0.7$ (see below). In all calculations it is assumed that the zeroth bond is perpendicular to the interface. The chain length is 6 bonds (corresponding to an alkyl chain of ~22 bonds).

Armed with $P(a)$, we can calculate any desired single chain property, e.g., order parameter profiles along the chains or along the micelle radius, spatial distributions of the various chain segments, average chain dimensions, chain free energies, entropy, etc. We have chosen to show here bond order parameter profiles and chain-free energies. The bond order parameters are directly related to measurable quantities and provide a sensitive means for testing the theory. The chain-free energies are important for determining the relative stability of different aggregates. In the existing models of amphiphile self-assembly, it is assumed that they are constant.^{1,2}

In Figure 2, we show the bond order parameters, S_k , of chains packed in spherical, cylindrical and planar aggregates for different values of the core radius, L . k denotes the bond connecting the k -th and $(k+1)$ -th chain segments. Also shown, in order to emphasize the effects of dense packing, are the order parameters of a 'free chain'. We use this term to describe a hypothetical case of a single chain in a micelle, anchored to the interface and confined to the core but without neighbors, i.e., the free chain is not subjected to (2). Its $P(a)$ is given by (6) with all $\lambda_i = 0$ ($\alpha_i = 1$). In other words, for the free chain $P(a) \propto \omega(a)$. In our calculations for planar bilayers, the chains are allowed to cross the mid-plane. The effects of

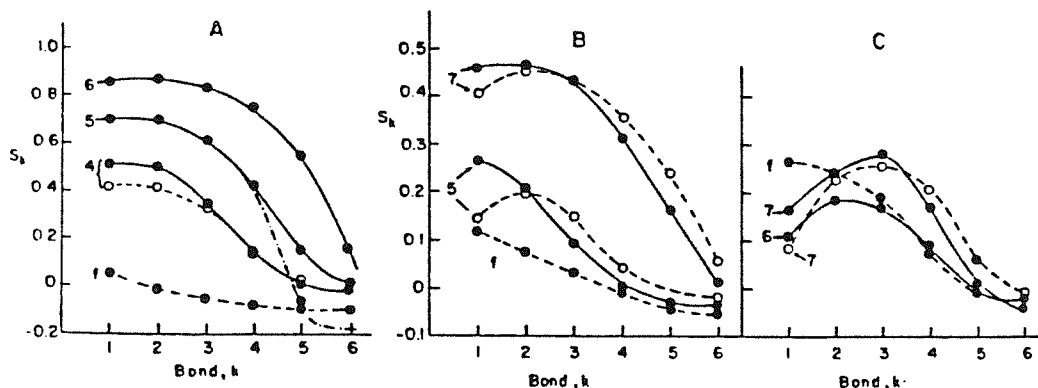


Figure 2: Bond order parameters S_k of 6-bond ('cubic') chains in planar bilayers (A), cylindrical micelles (B) and spherical micelles (C). L measures the radius (thickness) of the aggregate, see Figure 1. The curves marked "f" correspond to 'free chains', i.e., isolated chains with no neighbors around; these results are for $L=7$ but the properties of free chains are about the same for all $L \geq 3$. The open symbols are for freely flexible (equienergetic) chains. The dot-dashed line in A is for chains which are (artificially) forbidden to cross the bilayer's mid-plane.

artificially forbidding this 'inter-digitation' are shown by the dot-dashed curve in Figure 2A.

The main features observed in Figure 2 are as follows:

(i) For all geometries, the order parameters decrease towards the chain end. In the case of spheres, S_k first increases and then decreases. We believe that this is an artifact of the restriction that the zeroth bond must be perpendicular to the interface, thereby increasing the tendency of the next bonds to be lateral (lower S_k), in order to fill the volume available near the micelle's surface. By increasing the value of γ_h (for spheres) the maximum in S_k may be 'flattened'. Yet, such a modification would serve no purpose as we recognize in any case that the chain model is approximate. Note also that we have used the same value, $\gamma_h = 0.7$ for all geometries. (This value ensured that $S_1 = S_2$ for $L=5$ in bilayers).

(ii) The absolute value of S_k increases with L , i.e., as the average area per head-group decreases. This holds for all geometries. Moreover, the minimal area per head-group increases with surface curvature (the maximal radius corresponds to $L-n$ implying $m_1 = 1:2:3$ for bilayers, cylinders, and spheres, respectively).^{17,18} Hence, we should expect lower order parameters in spheres compared to cylinders and in cylinders compared to bilayers, as indeed revealed by Figure 2 and in agreement with experiment and other studies.^{5,6,14-17}

(iii) The role of internal energies in determining the shape and the extent of chain ordering is secondary, compared to effects of the geometrical packing constraints. This is demonstrated by the similarity between the curves corresponding to $\gamma, \gamma_h = 0.3, 0.7$ and $\gamma = \gamma_h = 1$; the latter case describes chains with zero kink energy, $\chi = 0$.

(iv) In spheres, S_k is quite similar to that of a free chain. On the other hand, in bilayers, marked differences between the order parameter profiles of constrained and free chains are observed. In cylinders the behavior is intermediate. In other words, the packing constraints become less stringent as the curvature of the interface increases. The qualitative explanation of this trend is quite simple: The average shape of a free chain is roughly that of a hemispherical globule attached to the interface. When packed in a bilayer, i.e., in the presence of close-by molecules, the chain is substantially squeezed, mainly near the interface, leading to an increase in the order parameters. The decline in S_k towards the chain end is due to terminations.¹⁴ The probability of chain termination increases towards the bilayer's midplane. When one chain terminates its neighbors must bend in order to fill volume, implying a decrease in the order parameter. The decrease in S_k is observed in the last few bonds because these bonds can approach and reach the midplane. (If, artificially, the chains are not allowed to cross the midplane they must point laterally once they arrive there. For 'cubic' chains, this implies a negative order parameter: see Figure 2.)

As noted above, the extent to which a free chain must be distorted in order to be packed in a spherical micelle is small. The higher order parameter of the free chain in this geometry, compared to planar bilayers, should be mainly attributed to the concave interface which (weakly) aligns the chains towards the center. The effect is diminished towards the chain end. In a micelle, some chains must reach the center. These chains are extended and thus lie along the normal to the interface. Yet, due to the sharp decrease in the volume available, only a tiny fraction of the chains actually reach the center: hence, their contribution to S_k is negligible.

Figure 3a shows $\bar{A}/kT = -\ln z$ for spheres, cylinders and bilayers, as a

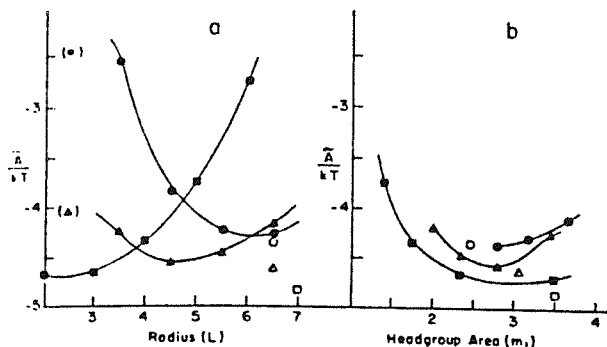


Figure 3: The average conformational free energy per chain as a function of: (a) the micellar radius (bilayer's half-thickness, (b) the average area per head group. Squares - planar bilayers, triangles - cylinders, circles - spheres. The open symbols are for free chains (L=7). The results are for 6-bond (7-segment) cubic chains, see Figures 1 and 2.

function of the aggregate's radius. Figure 3b shows the same results as a function of the (dimensionless) average area per head group, m_1 . Separate calculations of \bar{E} and \bar{S} (not shown) reveal that the minima and the overall shape of the free energy curves are predominantly determined by \bar{S} . Thus the packing constraints are more important than internal energies in determining the chain's free energy. The results in Figure 3 are very similar to those obtained by Gruen.¹³ In general, Figure 3 shows that as far as the chains (and not the head-groups) are concerned, the optimal aggregate thickness decreases with the curvature of its interface. Figure 3b shows that the optimal radius occurs at about the same m_1 value for all geometries. The differences in the minimal values of \bar{A} in the three geometries are small, ~ 0.1 kT. As mentioned previously, these differences are ignored in the conventional descriptions of amphiphile aggregation. It should be noted, however, that they are on the order of the variations in the amphiphile's standard chemical potential^{1,2,3,8} which are usually attributed solely to the 'opposing forces'^{1,2} acting at the micellar surface.

DISCUSSION

The statistical properties of chains packed in amphiphilic aggregates of various geometries have been explicitly studied using three theoretical, 'single chain', approaches. We refer to the models proposed by Gruen,¹¹⁻¹³ by Dill and Flory¹⁴ (DF) and by us^{17,18} as outlined in the previous section. The theories of Dill and Cantor^{15,16} and Dill and Flory¹⁴ share some important common ideas. Yet they also differ in some important respects, as we shall see. This section is devoted to a comparison of the various theories.

Gruen proposed¹¹ that the singlet distribution of chain conformations is given by a Boltzmann-like expression, $P(a) \propto \exp[-\beta f(a)]$, where $f(a)$ represents the effective energy of the chain in the aggregate. Using simplified notation, $f(a)$ is given by

$$f(a) = \epsilon(a) + w(a) + \sum_{k=1}^n \pi(r_k) A_k(a, r_k) \quad (22)$$

where $\epsilon(a)$ is the internal energy of a chain in conformation a and $w(a)$ is a term accounting for chain-water contact. $w(a) = 0$ if all chain segments are embedded within the hydrophobic core and increases, roughly linearly, with the number of segments protruding into the solution. The sum in (22) runs over all chain segments k . r_k denotes the distance of the k -th

segment from the interface or, alternatively, from the aggregate's center (mid-plane). $A_k(a, r_k)$ is the area occupied by the segment and $\pi(r)$ is the 'lateral pressure profile'. In the computations, $\pi(r)$ is treated as a discrete variable, π_1 . Namely, the core is divided into parallel layers (though not equidistant as in Figure 1), with a different π_1 for each layer. The areas $A_k(a, r_k)$ are calculated by a rather involved procedure which is not relevant to the present discussion.

The similarity of Gruen's pdf to the one given by (6) and (9) is apparent. In fact, using the discrete representation, π_1 instead of $\pi(r)$, (22) can be expressed as

$$f(a) = c(a) + w(a) + \sum_{i=1}^L \pi_1 \sum_{k \in i} A_k(a, r_k) \quad (23)$$

where the first sum is over all layers and the second is over all segments which are located partly or completely in layer 1. If we assume, (as in our treatment) that every segment 'belongs' fully to one layer (where its center is located) then, of course, the second sum is simply proportional to the quantity $\phi_1(a)$ defined in section 2. Actually, we may replace $\sum A_k$ by $\phi_1(a)$ and absorb the proportionality constant into π_1 which is treated as a parameter anyhow. This yields

$$P(a) \propto \exp\{-\beta[c(a) + w(a) + \sum_{i=1}^L \pi_1 \phi_1(a)]\} \quad (24)$$

which is identical to (6) provided one assumes $w(a) = \infty$ for conformations protruding beyond the interface and $w(a) = 0$ otherwise. The latest calculations of Gruen¹³ are based on an expression which is entirely equivalent to (24) and should thus be very similar to those derived from (6); see below.

The singlet pdf originally proposed by Gruen is in the spirit of Marcelja's mean field theory of chain ordering in bilayers and nematic fields.²⁵ Also, in both treatments the distribution parameters are determined by an iterative procedure based on a self-consistency requirement. In Gruen's model, the parameters are the π_1 's and the self-consistency condition is that the density within the hydrophobic core should be liquid-like. Technically, this method is different from our procedure, which consists of solving the algebraic equations of constraints, (8). In practice, however, the results should be the same, because (8) is nothing else but the requirement for uniform, liquid-like density. We have recently extended the application of our theory from the model chains described in the previous sections to 'real' (rotational isomeric state model) chains. To demonstrate the similarity between Gruen's results and ours, we show in Figure 4 the C-D bond order parameters of a $-(CH_2)_8-CH_3$ chain in a bilayer where the average area per head group is $25A^2$. It is clearly seen that the results are practically the same. The small differences are due to the different choices of $w(a)$ and to different averaging over configurations of the first bond. The figure also shows the results of magnetic resonance experiments²⁹ and molecular dynamics simulations.¹⁹ The agreement is excellent.

The theory of Dill and Flory (DF)¹⁴ and its later version, the Dill-Cantor (DC) theory,^{15,16} are based on a lattice model. Both are 'single-chain' theories in which the lattice is used to classify the possible chain conformations, to express packing constraints, and to introduce the concept of directionality. The basic physical assumptions underlying these theories are similar to those mentioned in section 2.

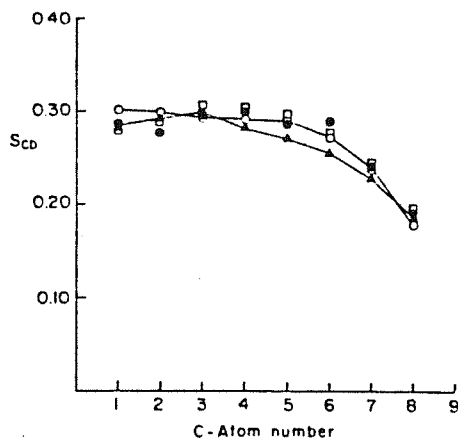


Figure 4: C-D bond order parameters for $-(\text{CH}_2)_8\text{-CH}_3$ chains in a planar bilayer as a function of the carbon atom along the chain. Solid circles - experimental data (ref. 29). Open circles - calculations based on equation (6) for rotational-isomeric-state chains, see Figure 1. Triangles - molecular dynamics simulations (ref. 19a). Squares - Gruen's calculations (refs. 12,13). All the computed results are for the same head-group area per chain (25\AA^2), gauche energy (700 cal/mole deg) and temperature (300K).

Namely, it is assumed that the density within the hydrophobic core is liquid-like and that the hydrocarbon-water interface is smooth.

The DF and DC theories describe the core of a planar bilayer by a regular cubic lattice. Spherical and cylindrical micelles are described by 'bent' cubic lattices, as shown in Figure 5. In all geometries, all lattice cells have the same volume. The layer width is ~ 3.6 bonds of an all-trans polymethylene chain, so that when all lattice sites are occupied, the core's density is liquid-like,¹⁴⁻¹⁶ as explained in the previous section. Each chain conformation is characterized by a sequence of 'walks' (bond placements) between nearest-neighbor sites on the lattice. Using i as the layer's index, we shall use the terms 'lateral', 'downward', and 'upward' bonds for those which connect a site in layer i with sites in layers i , $i+1$ and $i-1$, respectively. Thus, the lattice is used to define

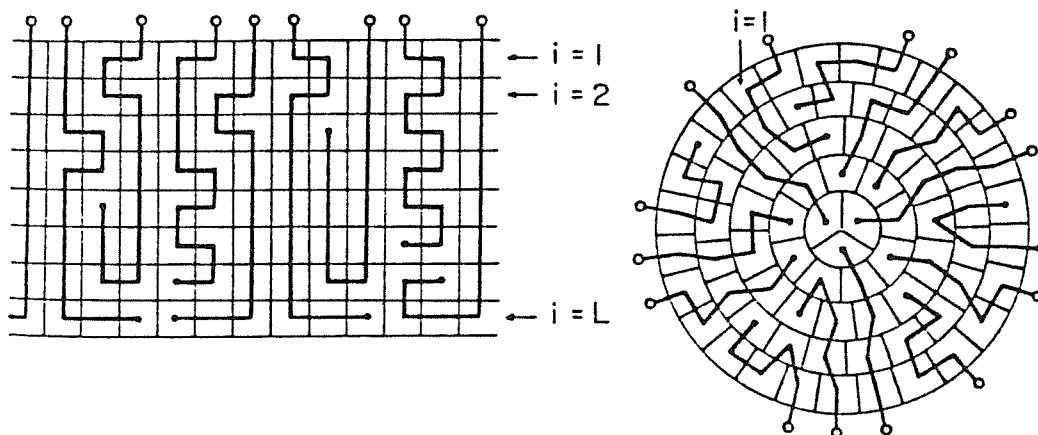


Figure 5: A two-dimensional representation of the Dill-Flory lattices¹⁴ describing planar bilayers and spherical/cylindrical micelles. Note the different bond angles corresponding to the different geometries. (Compare with Figure 1 where the bond angles are the same).

'directionality' (or 'order') with respect to the interface. All $i + 1$ bonds are regarded as parallel to the interface whereas the $i+1+i$ bonds are assumed perpendicular to it. In both the DF and DC theories, upward transitions (which imply chain 'reversals' toward the interface) are neglected. Hence, the chains can only propagate laterally or towards the center.

In the DF theory it is assumed that the chains obey Markovian statistics: Every lateral bond in layer i is assigned a probability q_i , regardless which bond it is along the chain. Correspondingly, the probability of a 'downward' ($i+1+i$) bond is $p_i=1-q_i$. Since chain reversals are ignored, every conformation can be specified by r_1, r_2, \dots, r_L where r_i is the number of lateral placements in layer i . More precisely, the sequence r_1, \dots, r_L specifies a group of conformations because every lateral step can occur in several directions. The probability of this group is expressed as

$$P_{DF}(r_1, \dots, r_L) = q_1^{r_1} p_1 q_2^{r_2} p_2 \dots q_L^{r_L} \quad (25)$$

where l is the 'deepest' layer reached by the chain. Note that $r_1 + r_2 + \dots + r_l + (l-1) = n-1 =$ number of bonds. (We keep using n for the number of chain segments.) Note that if the first lateral bond in layer 1 has Z_{11} possible directions, the second bond can point in $Z_{11}-1$ directions. (The number of allowed directions for the subsequent bonds depends on the lattice. For the regular cubic lattice, $Z_{11}=4$.) In writing (25), one ignores this change in the number of bond directions. Another assumption made in (25) is that all conformations are equi-energetic (freely 'flexible' chains,¹⁶ corresponding to $w(a)=1$ in (6)). The evaluation of the q_i 's is discussed below.

In the DC theory, the assumption of Markovian statistics, as well as the last two approximations, are removed. But, to facilitate the comparison between the DF, DC theories and ours, we shall first consider only the 'flexible chain limit' of all these approaches. (Chain energies play an important role in the DC theory, [see below]). In this limit, the pdf proposed by Dill and Cantor is

$$P_{DC}(r_1, \dots, r_L) = g_{DC}(r_1, \dots, r_L) = \xi_1^{r_1} \xi_2^{r_2} \dots \xi_L^{r_L} / \Xi \quad (26)$$

The partition function Ξ ensures normalization of $P(r_1, \dots, r_L)$, subject to summation over all possible r_1, \dots, r_L . Each ξ_i represents the statistical weight assigned to a lateral bond (in any direction) in layer i . The statistical weight of all downward steps is set equal to 1. The evaluation of the ξ_i 's is considered below. The spatial degeneracy factor g can be expressed as

$$g_{DC}(r_1, \dots, r_L) = Z_{11}^{h(r_1)} (Z_{11}-1)^{r_1-1} Z_{22}^{h(r_2)} (Z_{22}-1)^{r_2-1} \dots \quad (27)$$

where $h(r_i) = 1$ if $r_i \geq 1$ and 0 otherwise. This form accounts for the variation of the lateral coordination number with r_i . (It does not account for high-order self-avoided walks, but for short chains this is a very good approximation.) In the calculations^{15,16}, $Z_{11} = Z = 4$ for all geometries. Furthermore, for all geometries, the vertical coordination numbers $Z_{i,i+1}$ were set equal to 1 (see below).

In reference 17 we applied our pdf (6) to chains which are compatible

with the DF lattices shown in Figure 5. We assumed that all chain conformations are equi-energetic. One reason was the different bond angles implied by the different lattices. This prevents a consistent assignment of a single kink energy for all geometries. (Note that in the curved lattices the bond angles are not uniquely defined.) Chain reversals, (i.e., upward bond placements) were taken into account, but their effect on order parameter profiles and other properties was found to be minor.¹⁷ In particular, we found that the bond-order parameters in spherical and cylindrical micelles decrease along the chain, in qualitative agreement with experimental data^{5,6} and with Gruen's calculations.¹¹⁻¹³ The behavior is similar to that of the model chains considered in the previous section,¹⁸ cf. Figures 1,2. On the other hand, the DF model¹⁴ predicts that in curved micelles S_k increases with k (see below). (In the DC model, agreement with the observed behavior of S_k is obtained provided the chains are assigned finite kink energies; but for entirely flexible chains, S_k still increases with k).¹⁶ These different predicted behaviors of S_k reflect conceptual differences between the theories. To explore them let us first cast (6) into a form which is more appropriate for comparison with (25) and (26).

In section 2, we have use ϕ_i to denote the number of chain segments in layer i . One can write $\phi_i = D_i + R_i + U_i$ where D_i is the total number of segments 'arriving' in layer i following downward ($i-1+i$) bonds. R_i is the number of $i+i$ bonds and U_i is the number of upward ($i+1+i$) bonds. In the DF and DC theories $U_i=0$, and we shall therefore adopt the same assumption here. Note that $D_1=N$. $U_1=0$ implies that the number of chains terminating in layer i is $T_i = D_i - D_{i+1}$.^{14,17} Using (1) it is easily verified that

$$R_i = M_i - N - \sum_{j=1}^{i-1} T_j \quad i=1, \dots, L \quad (28)$$

or after division by N

$$\langle r_i \rangle = (m_i - 1) - \sum_{j=1}^{i-1} t_j \quad i=1, \dots, L \quad (29)$$

where $t_j = \langle d_j \rangle - \langle d_{j+1} \rangle$ is the probability for chain termination in layer j . $\langle d_j \rangle$ is the probability that the chain will make an $i-1+i$ transition. [$d_j(a)=1$ if the chain reaches j , and 0 otherwise: $\langle d_j \rangle \equiv 1$.] Clearly (29) is entirely equivalent to (2), provided we identify $\phi_i(a) = d_i(a) + r_i(a)$. ($\langle \phi_i \rangle = \langle d_i \rangle + \langle r_i \rangle$, as appropriate for chains without reversals ($u_i \equiv 0$)).¹⁷ Using $\phi_i = d_i + r_i$, we also find that after grouping together all conformations with the same r_1, r_2, \dots, r_L (6) reduces to

$$P(r_1, \dots, r_L) = g(r_1, \dots, r_L) \alpha_1^{r_1} \alpha_2^{r_2+1} \alpha_3^{r_3+1} \dots \alpha_L^{r_L+1} / z \quad (30)$$

where we have set $\omega(a)=1$ (flexible chains). The α_i 's here are the same as those defined in eq. (6); a factor of α_1 , which is common to all conformations, has been cancelled out ($d_1 \equiv 1$).

The form that we have used for the degeneracy factor is¹⁷

$$g(r_1, \dots, r_L) = Z_{11}^{h(r_1)} (Z_{11} - 1)^{r_1-1} Z_{12} Z_{22}^{h(r_2)} (Z_{22} - 1)^{r_2-1} Z_{23} \dots \quad (31)$$

When $Z_{i,i+1} = 1$, this form reduces to (27). In the regular cubic lattice describing a planar bilayer, every site in layer i has one nearest neighbor

in $i+1$, i.e., the 'downward' coordination number is, indeed, $Z_{i,i+1} = 1$. On the other hand, in the curved lattices (Fig. 5), the corresponding number of neighbors is ('on the average') $Z_{i,i+1} = M_{i+1}/M_i$ where M_i is the number of sites (total volume) in i . (Similarly, for $i+i-1$ transitions, we have used $Z_{i,i-1} = M_{i-1}/M_i$). This choice accounts for the decrease in volume towards the center in the curved geometries. In our opinion, this is the most obvious and natural choice for $Z_{i,i\pm 1}$. We shall see below, however, that the numerical results derived from (30) and (31) are quite insensitive to the choice of $Z_{i,i+1}$.

All the distribution parameters, the q_i 's in (25), the ξ_i 's in (26) and the α_i 's in (30) are determined by the packing constraints (29). ((29) is equivalent to $\langle \phi_i \rangle = \langle d_i \rangle + \langle r_i \rangle = m_i$.) The evaluation of the q_i 's is particularly simple due to the Markovian character of (25), which is reflected by the fact that q_i, p_i is a pair of normalized conditional probabilities. This property, together with the neglect of chain reversals, allow one to cast the DF theory in an elegant and simple matrix formulation.¹⁴ In particular, by direct substitution of (25) into (29), it can be shown¹⁴ that the equation for $i=1$ involves only q_1 . (The exact equation is $q_1 + q_1^2 + \dots + q_1^{n-1} = m_1 - 1$ where $n-1$ is the number of bonds.) The equation for $i=2$ includes only q_2 and the previously determined value of q_1 ($t_1 = q_1^{n-1}$). In general, the i -th equation can be solved for q_i using the known values of q_1, \dots, q_{i-1} . This sequential determination of the q_i 's is a direct consequence of: (i) the neglect of reversals and (ii) the Markovian approximation. Since (26) and (30) are both non-Markovian distributions, all the ξ_i 's and α_i 's appear in all the equations of constraints (29). To determine the values of these parameters, (29) should be solved for all layers 'simultaneously'.

In (26) and (30), the ξ_i 's and α_i 's, respectively, are statistical weights rather than conditional probabilities. The difference between these two concepts and its implication with regard to chain statistics are discussed in detail elsewhere.²⁶ To demonstrate its consequences in the present context, one example will suffice. Consider, for instance, the (overall) probability, $P(r_1)$ of r_1 lateral bond placements ($r_1 < n-1$) in layer 1. It can be shown that the DF distribution (25) implies $P(r_1) = q_1^{r_1} p_1 = q_1^{r_1} (1 - q_1)$. On the other hand, (26) and (30) yield, respectively, $P(r_1) = \xi_1 W_A(r_1)$ and $\alpha_1^{-1} W_B(r_1)$. $W_A(r_1)$ and $W_B(r_1)$ are (different) functions of r_1 and reflect the total statistical weight of all possible conformations of the $(n-1)-r_1$ bonds following the first r_1 bonds. In the Markovian approximation this statistical weight is set equal to 1. More generally, in this approximation the probability of finding a given bond in a given 'state' depends only on the previous bonds, whereas this is not so according to (26) or (30).

There are some 'technical' differences between the DC distribution and ours, such as the expressions used for $g(r_1, \dots, r_L)$. But there is one conceptual difference which is clearly reflected by comparing (26) and (30). In (30), and more generally in (6), we assign the same statistical weight to all chain segments in layer i , regardless of whether they are the tips of lateral or downward (or upward) bond placements. In our derivation of (6), this is a direct consequence of the packing constraints. Chain ordering, i.e., the tendency of the bonds to align along the normal to the interface, is a consequence of the packing constraints. On the other hand, in the DF and DC theories, this tendency is built into the pdf's via the lattices described in Figure 5, and the assignment of different statistical weights to lateral and downward bond placements. The constraints are then used to determine the numerical values of the statistical weights. To clarify this point, suppose we try to extend the DF (or DC) treatments by allowing upward, $i+i-1$ bond placements. This would require, in addition to p_i and q_i (or ξ_i and 1) another probability, say s_i , for an $i+i-1$

transition, so that now $p_1 + q_1 + s_1 = 1$. Clearly, the packing constraints are not sufficient for determining all p_1, q_1, s_1 -- an additional assumption is required ($s_1 = p_{1-1}$ is a reasonable one because both describe $i-1 \leftrightarrow i$ bonds). Additional or alternative assumptions would be needed if the chains do not conform to the special lattices of Figure 5 (cf. Figure 1). In this case a natural extension would be to assign a probability $p_1(\theta)$, or a statistical weight $\xi_1(\theta)$, for bonds located in layer 1 and oriented by an angle θ with respect to the normal to the interface. Again, an assumption regarding the θ -dependence of these functions will be needed. This is actually quite similar to Marcelja's treatment of chain ordering in bilayers and nematic solvents.²⁵ (His choice was $\xi_1(\theta) \propto \exp[-\beta \eta_1 P_2(\cos \theta)]$ where η_1 is proportional to the order parameter in layer 1. This is based on an extension of the Maier-Saupe mean-field theory of nematic liquid crystals³⁰).

The total number of α_i factors in (30) is a constant: $r_1 + r_2 + \dots + r_L + (L-1) = n-1$. On the other hand, in (26) the number of ξ_i factors depends on L -- the deepest layer reached by the chain [this number is $(n-1) - (L-1)$]. In (25) the number of p_i, q_i factors is a constant $(n-1)$ but, again, we should expect different results because of the Markovian character of (25). To demonstrate the differences, we show in Figure 6 bond-order parameter profiles calculated by the various methods for 4-segment (3-bond) chains; all are compatible with the DF-lattices (Figure 5). These very short model chains represent alkyl chains of ~ 11 C-C bonds. S_k values calculated on the basis of (26) are shown for flexible (equi-energetic) and 'real' chains in cylindrical micelles only -- the results were taken from reference 16. It is clearly seen that our pdf (30) predicts that S_k decreases with k for all geometries -- even for entirely flexible chains. On the other hand, the DF and DC theories predict that for flexible chains in curved aggregates S_k increases with k . According to the DC theory¹⁶ this behavior is reversed when chain internal energies are taken into account. (The results shown in Figure 6b are obtained using $\gamma = \exp(-8\chi) = 0.3$ where χ is the kink energy). This finding is inconsistent with our conclusion of the previous section according to which S_k , as well as other chain properties, are dominated by packing constraints with energetic effects playing only a secondary role.

Figure 6 also shows two other sets of results. In one case we have used (30) but with 'simplified' degeneracy factors, namely, with all $Z_{1,i+1} = 1$, cf. (31). (In this approximation we obtain (27)). The results clearly demonstrate that this modification has no qualitative consequences regarding the behavior of S_k . The other set of results corresponds to an approximate pdf obtained via sequential maximization of S , cf. section 2. Since the derivation is quite lengthy, we shall omit most of the details and suffice in mentioning the basic steps. One can write $P(r_1, r_2, \dots) = P(r_1)P(r_2|r_1)P(r_3|r_1, r_2) \dots$ where $P(r_i|r_1, \dots, r_{i-1})$ is the conditional probability of r_i lateral bonds in layer i following r_1, \dots, r_{i-1} such steps in the previous layers. This decomposition implies an analogous decomposition of S into layer entropies: $S = S_1 + S_2 + \dots + S_L$ where S_1 involves only $P(r_1)$, S_2 involves only $P(r_1)$ and $P(r_2|r_1)$, etc. The next step consists of maximizing S_1 subject to the first ($i=1$) constraint in (29). Then S_2 is maximized subject to the $i=2$ constraint and so on. This procedure leads to a pdf of the form

$$P_S(r_1, \dots, r_L) = P(r_1)P(r_2|r_1)P(r_3|r_1, r_2) \dots$$

$$= \frac{[g(r_1)\alpha_1^{r_1}]}{z_1} \frac{[g(r_2)\alpha_2^{r_2}]}{z_2(r_1)} \frac{[g(r_3)\alpha_3^{r_3}]}{z_3(r_1, r_2)} \quad (32)$$

in which every factor in square brackets is separately normalized, e.g.

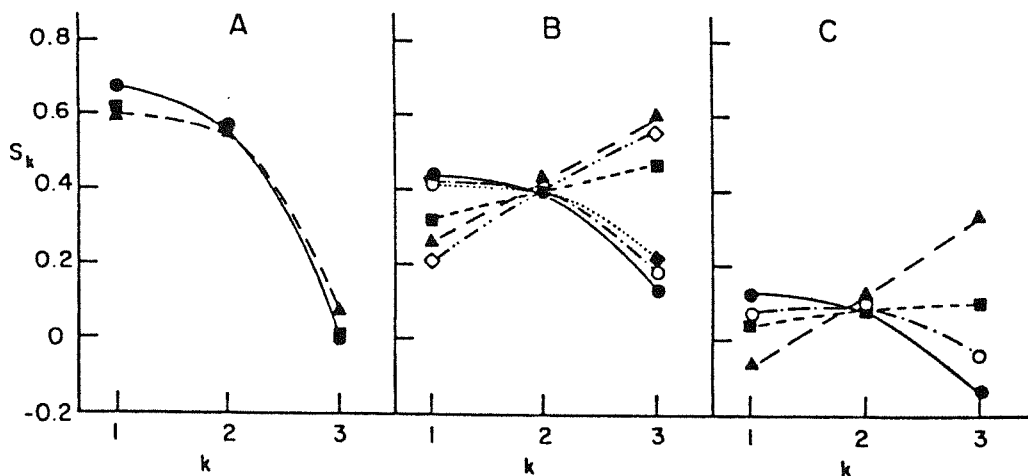


Figure 6: Order parameter profiles for 3-bond (4-segment) model chains compatible with the DF-lattices of Figure 5, calculated using several different models. A) Planar bilayer ($L=3$, $m_1=1.33$); B) Cylinders ($L=4$, $m_1=1.75$); C) Spheres ($L=4$, $m_1=2.31$). (●) -- calculated using equation (30) with degeneracy factor given by (31). (○) -- equation (30) with degeneracy factor given by (31) but with $Z_{1,i+1}=1$ (i.e., the same g as in (27)). (■) -- according to the DF model (25). (▲) -- equation (32), i.e., according to the sequential maximization procedure. For cylinders, we also show results derived from the DC distribution (ref. 16), equation (26): (◆...◆) -- partially flexible ('stiff') chains; (◇----◇) -- flexible chains.

$z_2(r_1)$ is the sum of $g(r_2)\alpha_2 r_2^2$ over all $0 \leq r_2 \leq (n-1)-(r_1-1)$. $g(r_1)$ is the number of sequences of r_1 lateral bonds. It is not difficult to show that when (32) is substituted into (29) the $i=1$ equation involves only α_1 , the $i=2$ equation involves α_1, α_2 and so on. Thus, in analogy to the DF-procedure, the α_i 's are evaluated sequentially. Note also that: (i) in (32), just like in (25), the vertical coordination numbers $Z_{i,i+1}$ are set automatically equal to one; and (ii) the number of α_i factors in P_S is equal to the sum of lateral bonds (and not to $n-1$). The order parameters calculated using (32) show the same qualitative behavior predicted by (25) and (26), i.e., S_k increases with k for the curved geometries, the increase being steepest for (32).

CONCLUDING REMARKS

In the theory presented in section 2, we explored the factors determining chain organization in micellar aggregates of various geometries. Based on two different approaches, we derived (the same) probability distribution function of chain conformations within an aggregate. All the assumptions and approximations involved in the derivation have been explicitly stated. Some of those may be controversial and will be examined in more detail in the near future, e.g., the assumption that the hydrocarbon-water interface is smooth.

In section 3 our single-chain (mean field) theory has been applied to approximate model chains; the predictions are in good qualitative agreement with experimental data. In section 4 it was demonstrated that when applied to a more realistic chain model the agreement with experiment and computer simulation results is quantitative. In a sense, the agreement with the molecular dynamics data is more meaningful, theoretically at least, as it enables us to compare single chain and many-chain calculations for systems with well defined parameters (including smooth interface, etc.). We

believe that the good agreement with the many-chain simulations is valid for all single-chain properties such as order parameter profiles and spatial distributions of chain segments. This is supported as well by Gruen's calculations.¹³ Of course, molecular dynamics simulations also provide information on cooperative phenomena and dynamical properties, which static single-chain theories cannot treat.

The last section has been devoted mainly to a comparison with other single chain models. We have shown that the pdf of chain conformations proposed (independently) by Gruen,¹¹⁻¹³ particularly in its latest version,¹³ is essentially the same pdf that we have derived in section 2. The similarities and differences between our approach and those of Dill-Flory and Dill-Cantor have been discussed in detail. The differences here pertain to some of the basic assumptions as well as to some different conclusions regarding chain statistics. Most significantly, while Dill and Cantor¹⁶ find that chain stiffness plays a central role in determining chain ordering in curved micelles, we find this effect to be only secondary.

ACKNOWLEDGEMENTS

A. B.-S. thanks the Fund for Basic Research, administered by the Israel Academy of Sciences and Humanities. The Fritz Haber Research Center is supported by the Minerva Gesellschaft für die Forschung, mbH, München, BRD. W. M. G. thanks the National Science Foundation and the ACS-Petroleum Research Fund for financial support.

REFERENCES

1. C. Tanford, "The Hydrophobic Effect", 2nd edition, Wiley, New York, 1980.
2. a) J. N. Israelachvili, D. J. Mitchell and B. W. Ninham, *J. Chem. Soc. Faraday Trans. 2*, **72**, 1525 (1976).
b) J. N. Israelachvili, S. Marcelja and R. G. Horn, *Quart. Rev. Biophys.* **13**, 121 (1980).
c) J. N. Israelachvili, these proceedings, and in "Physics of Amphiphiles: Micelles, Vesicles and Microemulsions", P. P. V. Degiorgio and M. Corti, Editors, North Holland, 1984.
3. See, e.g., E. Vikingstad and H. Høiland, *J. Colloid Interface Sci.* **64**, 510 (1978).
4. See, e.g., (a) E. T. Samulski, *Ferroelectrics* **30**, 83 (1980),
(b) A. Ben-Shaul, Y. Rabin and W. M. Gelbart, *J. Chem. Phys.* **78**, 4303 (1983).
5. a) B. Mely, J. Charvolin and P. Keller, *Chem. Phys. Lipids* **15**, 161 (1975).
b) J. Charvolin, *J. Chem. Phys.* **80**, 15 (1983).
c) J. Charvolin and Y. Hendrikx, in "NMR in Liquid Crystals", J.W. Emsley and G. Luckhurst, Editors, Reidel Publishing Co., in press.
6. a) H. Walderhaug, O. Soderman and P. Stilbs, *J. Phys. Chem.* **88**, 1655 (1984).
b) B. Lindman, T. Ahlñäs, O. Soderman and H. Walderhaug, *Faraday Disc. Chem. Soc.* **76**, 317 (1983).
c) T. Ahlñäs, O. Soderman, H. Walderhaug and B. Lindman, In "Surfactants in Solution", Vol. 1, K.L. Mittal and B. Lindman, Editors, p. 107, Plenum Press, New York, 1984.
7. For a review see, J. F. Nagle, *Ann. Rev. Phys. Chem.* **31**, 157 (1980).
8. a) F. M. Menger, *Acc. Chem. Res.* **12**, 111 (1979).
b) P. Fromherz, *Chem. Phys. Lett.* **77**, 460 (1981).

- c) B. Cabane, *J. Phys. Paris*, 42, 847 (1981).
9. T. Zemb and C. Chachaty, in "Surfactants in Solution", K.L. Mittal and B. Lindman, Editors, Vol. 1, Plenum Press, New York, 1984.
 10. B. Lemaire and P. Bothorel, *Macromolecules* 13, 311 (1980).
J. Polym. Sci., Phys. Ed. 20, 867 (1982).
 11. D. W. R. Gruen and E. H. B. de Lacey, in "Surfactants in Solution", K. L. Mittal and B. Lindman, Editors, Vol. 1, p. 279, Plenum Press, New York, 1984.
See also, D. W. R. Gruen, *J. Colloid Interface Sci.* 84, 281 (1981);
Biochem. Biophys. Acta 595, 161 (1980).
 12. D. W. R. Gruen, *J. Phys. Chem.* 89, 146, 153 (1985).
 13. D. W. R. Gruen, *Prog. Colloid Polymer Sci.* 70, 6 (1985).
 14. a) K. A. Dill and P. J. Flory, *Proc. Natl. Acad. Sci., USA*, 77, 3115, (1980).
b) *ibid.* 78, 676 (1981).
 15. a) K. A. Dill and R. S. Cantor, *Macromolecules* 17, 380 (1984).
b) R. S. Cantor and K. A. Dill, *Macromolecules* 17, 384 (1984).
 16. K. A. Dill, D. E. Koppel, R. S. Cantor, J. D. Dill, D. Bendedouch and S.-H. Chen, *Nature*, 309, 42 (1984).
 17. a) A. Ben-Shaul, I. Szleifer and W. M. Gelbart, *Proc. Natl. Acad. Sci. USA* 81, 4601 (1984).
b) in "Physics of Amphiphiles: Micelles, Vesicles and Microemulsions", V. Degiorgio and M. Corti, Editors, North Holland, 1984.
 18. a) A. Ben-Shaul, I. Szleifer and W. M. Gelbart, *J. Chem. Phys.* 83, 3597 (1985).
b) I. Szleifer, A. Ben-Shaul and W. M. Gelbart, *J. Chem. Phys.* 83, 3612 (1985).
 19. P. van der Ploeg and H. J. C. Berendsen, (a) *Mol. Phys.* 49, 233 (1983).
(b) *J. Chem. Phys.* 76, 3271 (1982).
 20. B. Owenson and L. R. Pratt, to be published.
 21. a) B. Owenson and L. R. Pratt, *J. Phys. Chem.* 88, 2905 (1984).
b) S. W. Haan and L. R. Pratt, *Chem. Phys. Lett.* 79, 436 (1981).
 22. J. M. Haile and J. P. O'Connell, *J. Phys. Chem.* 88, 6363 (1984).
 23. See, e.g., a) J. D. Weeks, D. Chandler and H. C. Andersen, 54, 5237 (1971).
b) J. A. Barker and D. Henderson, *Ann. Rev. Phys. Chem.* 23, 439 (1972).
c) A. Wulf, *J. Chem. Phys.* 64, 104 (1975).
d) W. M. Gelbart and B. Barbov, *Accts. Chem. Res.* 13, 290 (1980).
 24. a) E. T. Jaynes, in "Statistical Physics", Brandeis Lectures, K. W. Ford, Editor, Vol. 3, p. 182, Benjamin, New York, 1963.
b) R. D. Levine and M. Tribus, Editors. "The Maximum Entropy Formalism," MIT Press, Cambridge, 1979.
 25. S. Marcelja, a) *Biochem. Biophys. Acta* 367, 165 (1974).
b) *J. Chem. Phys.* 60, 3599 (1974).
 26. P. J. Flory, "Statistical Mechanics of Chain Molecules," Wiley, New York, 1969.
 27. M. A. Winnik, D. Rigby, R. F. T. Stepto and B. Lemaire, *Macromolecules*, 13, 699 (1980).
 28. P. J. Missel, N. A. Mazer, G. B. Benedek, C.Y. Young and M. C. Carey, *J. Phys. Chem.* 84, 1044 (1980).
 29. J. Seelig and W. Niederberger, *Biochemistry* 13, 1585 (1974).
 30. See, e.g., S. Chandrasekhar, "Liquid Crystals," Cambridge University Press, Cambridge, U.K., 1977.